ACS APPLIED MATERIALS & INTERFACES

Research Article

www.acsami.org

Curcumin–Cysteine and Curcumin–Tryptophan Conjugate as Fluorescence Turn On Sensors for Picric Acid in Aqueous Media

Bedanta Gogoi and Neelotpal Sen Sarma*

Physical Sciences Division, Polymer Laboratory, Institute of Advanced Study in Science and Technology, Guwahati, Assam 781035, India

Supporting Information

ABSTRACT: Rapid detection of picric acid in real sample is of outmost importance from the perspective of health, safety, and environment. In this study, a very simple and cost-effective detection of picric acid is accomplished by developing a couple of biobased conjugates curcumin–cysteine (CC) and curcumin–tryptophan (CT), which undergo efficient fluorescence turn on toward picric acid in aqueous media. Both the probes experience about 26.5-fold fluorescence enhancements at 70 nM concentration of the analyte. Here, the fluorescence turn on process is governed by the aggregation induced emission, which is induced from the electrostatic interaction between the conjugates with picric acid. The detection limit of CC and CT are about 13.51 and 13.54 nM of picric acid, respectively. Importantly, both the probes exhibit high selectivity and low interference of other analogues toward the detection of picric acid. In addition, the probes are highly photostable, show low response time and are practically applicable for sensing picric acid in real environmental samples, which is the ultimate goal of this work.

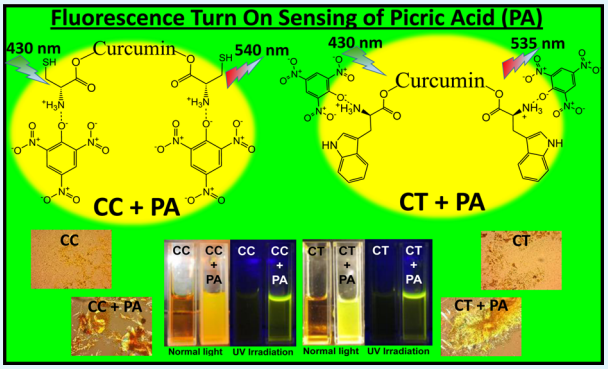

KEYWORDS: *curcumin, L-BOC cysteine, L-BOC tryptophan, fluorescence turn on, nitroaromatic chemicals, picric acid sensing, aggregation induced emission*

INTRODUCTION

2,4,6-Trinitrophenol, commonly known as picric acid (PA) is a nitroaromatic explosive chemical and is widely employed in deadly weapons. Its explosive power is reported to be superior to that of 2,4,6-trinitrotoluene (TNT).[1,2] It is also largely used in manufacturing rocket fuels, fireworks, matches, dyes, pharmaceutics, etc.[3,4] Niroaromatic chemicals (NACs) are electron withdrawing in nature and upon initiation can undergo highly exothermic reaction producing toxic gas vapors.[5] PA is water-soluble and hence its extensive use may increase the possibility to be released to the environment, which can finally leads to water and soil pollution. It is an environmentally deleterious chemical and potentially hazardous for wildlife and human health. Material safety data sheet reveals that it is very hazardous in case of skin and eye contact, ingestion, or inhalation. Severe overexposure can produce lung damage, choking, unconsciousness, or death. Therefore, innovation of methods for sensitive detection and removal of PA from the environment have attracted substantial research efforts in recent years. However, practically the real time detection of PA takes place in complex environments like mine fields, blast sites, transportation areas, wastewater treatment facilities, etc.[6,7] In such sites, the presence of other explosive chemicals along with PA are undefined. Under such situations, the sensitive and selective detection of PA becomes a very challenging task for the researchers. It is well-known that fluorescence technique is widely used for such purposes because of its high sensitivity, quick response, and easy sample preparation.[8,9] Also, it is common that fluorescence turn on signal for sensing application is superior to that of fluorescence turn off signal.[10,11] Literature study revealed that there are few reported research findings for selective detection of PA through fluorescence turn on signals.[10−13] Considering all these circumstances, we have developed two biobased materials curcumin–cysteine (CC) and curcumin–tryptophan (CT) by simple Fischer esterification reaction for efficient fluorescent turn on detection of PA in laboratory and real samples. Development of bio-based materials for such purposes is of great importance as the reported materials for fluorescence sensing of explosive chemicals are neither readily available are nor very eco-friendly. For example, conjugated polymers are considered as good contestant but its use often hampered because of multistep synthesis, low yield, and time-consuming nature.[7,14,15] Pyrene and its derivatives,[16] CdTe/CdS core/shell quantum dots (QDs),[17] hybrid CdTe QDs,[18] functionalized CdSe/ZnS QDs,[19] metal–organic framework [Cd(NDC)0.5-(PCA)]. G_x (G = guest molecules, NDC = 2,6-naphthalene dicarboxylic acid, PCA= 4-pyridinecaboxylic acid)[20] are also

Received: February 5, 2015
Accepted: May 8, 2015
Published: May 8, 2015

DOI: 10.1021/acsami.5b01102
ACS Appl. Mater. Interfaces 2015, 7, 11195−11202

reported for fluorescence sensing of explosive chemicals, but their routine use is discouraged because of their high toxicity to the environment. Most of such materials are efficient in organic media but insoluble/unstable in water and hence becomes unfeasible as far as practical use for the detection of explosive chemicals in real samples is concerned.[21,22] Recently, Sarkar et al. reported an efficient technique for detection of PA where a redox-switchable copper(I) metallogel was developed which possesses entangled fibrous network.[23] It forms an orange-red precipitate on exposure to PA due to breaking of the gel framework. In the present endeavor, we have used curcumin-amino acid conjugated systems for selective detection of PA in aqueous medium with lower limit of detection (LOD) and also applicable for real environmental samples. The method is based on simple electrostatic interaction between CC and CT with PA as represented in Scheme 1. Such interaction causes molecular aggregation that determines the fluorescence enhancement and generally called aggregation induced emission (AIE).[24]

Scheme 1. Schematic Illustration for the Electrostatic Interaction between CC and CT with PA Causing Fluorescence Turn On

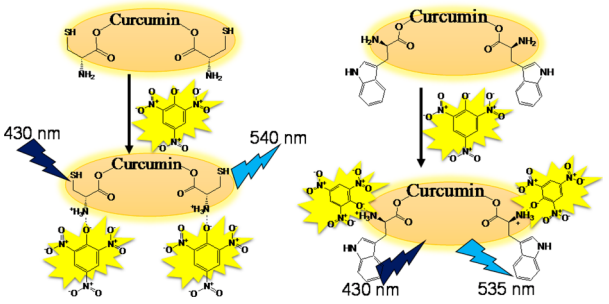

Curcumin [1,7-bis(4-hydroxy-3-methoxyphenyl)-1,6-heptadiene-3,5-dione] constitutes about 77% of the curcuminoids in the rhizomes of turmeric plant (*Curcuma longa*) and has tremendous medicinal properties.[25] On the other hand, cysteine (Cys) is a semiessential amino acid while tryptophan (Tryp) is an essential amino acid for human body. We have already reported that curcumin polymers are efficient in vapor sensing of PA, while its copolysulfone with hexane is an active biosensor for hemin, CT with CdTe quantum dot biohybrid has also been developed which has fluorescence activity toward bacterial DNA.[26−28] It was observed that CT and CC are very efficient in aqueous phase detection of PA. From the best of our knowledge, such materials for fluorescence turn on detection of PA in aqueous phase with very low LOD are not reported earlier. Also the probes reached about 26.5-fold increase in the fluorescence intensity which is significantly higher compared to the previously reported works.

EXPERIMENTAL SECTION

Materials. Curcumin, L-BOC cysteine and L-BOC tryptophan and PA were purchased from SIGMA. 2,5-dinitrosalisylic acid (DNSA), nitrobenzene (NB), *o*-nitrophenol (ONP), *p*-nitrophenol (PNP), *p*-toluene sulfonic acid (PsOH), HCl, nd methanol were purchased from MERCK. These chemicals were used without further purification. Trinitrotoluene (TNT) was provided by Forensic Laboratory, Guwahati-Assam. The chemical structure of the experimental NACs are shown in Scheme-2.

Scheme 2. Structure of the Experimental NACs

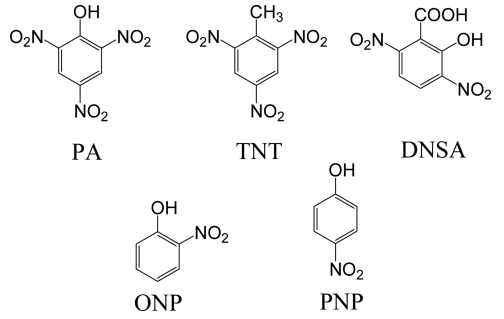

Caution! *PA and TNT should be stored with extreme caution. Personal protective equipment must be worn while handling such chemicals and also used in small quantities. PA is stored in 50% of water for safety reasons. The solubility of PA in water is 12.7 g/L. The OSHA permission exposure limit and the ACGIH threshold limit (TLV) for PA is 0.1 mg/m^3.*

Instruments and Characterization. Fourier transform infrared (FT-IR) spectra were recorded with the help of Nicolet 6700 FT-IR in the range of 650−4000 cm^{-1} in transmittance mode over 32 scans using ATR technique. The mass spectra of the samples were collected with the help of Thermo Dionex LC-MS using methanol as solvent. NMR analysis was performed using Bruker DPX-300 NMR spectrophotometer. The elemental distribution of the samples were determined with the help of Vario EL CUBE elemental analyzer. Electronic transitions of the experimental solutions were observed by monitoring the room temperature UV−vis spectra using Shimadzu (UV1601PC) spectrophotometer. Steady state fluorescence spectra were recorded using Varian Cary Eclipse fluorescence spectrophotometer with slit width of 2.5 nm at constant scan speed of 240 nm/s and with a detector voltage of 450 V. The experimental solutions were subjected to dynamic light scattering (DLS, Malvern Nano ZS90) for particle size and zeta potential measurements. Images of the vacuum-dried samples were collected using Zeiss Scope.A1 Optical Microscope. These samples were observed under fluorescence microscope (Leica DMI 3000 B fluorescence microscope) using a monochromatic light called rhodamine.

Procedure for Fluorescence Sensing of PA. Stock solutions (0.01 mM) of both CC and CT were prepared in double distilled water. Two milliliters of each solution were transferred into quartz cuvette (4 × 1 × 1 cm) with high vacuum Teflon stopcocks and the fluorescence spectra were recorded by applying excitation wavelength (λ_{ex}) of 430 nm.

Procedure for Fluorescence Sensing of PA in Real Sample. Tap water, pond water, and drinking water were used to prepare real samples. First, the waters were simply filtered and spiked with PA to prepare the analyte. Same instrumental parameters were used for the fluorescence sensing of PA in real samples.

RESULTS AND DISCUSSION

Synthesis. Synthesis of CT was published elsewhere.[28] L-BOC Cysteine was used for the synthesis of CC instead of L-BOC Tryptophan used for the synthesis of CT. The chemical reactions involved during the synthesis of CC are shown in Scheme 3. The synthesized compounds were spectroscopically characterized with the help of FT-IR (refer Supporting Information Figure S1), ^{1}H NMR and 13C-NMR (refer Supporting Information Figure S2A−C) and MS study (refer Supporting Information Figure S3) as described in the Supporting Information. The distribution of the elements viz. C, H, N, S and O were obtained with the help of elemental analysis as given in Supporting Information Table S1.

The photophysical properties of CC and CT were studied with the help of UV−vis absorption and fluorescence spectroscopy in aqueous media. Prior to the fluorescence

DOI: 10.1021/acsami.5b01102
ACS Appl. Mater. Interfaces 2015, 7, 11195−11202

Scheme 3. Chemical Reaction Involved during the Synthesis of (a) Curcumin−BOC Cysteine Conjugate, (b) CC, and (c) the Chemical Structure of CT

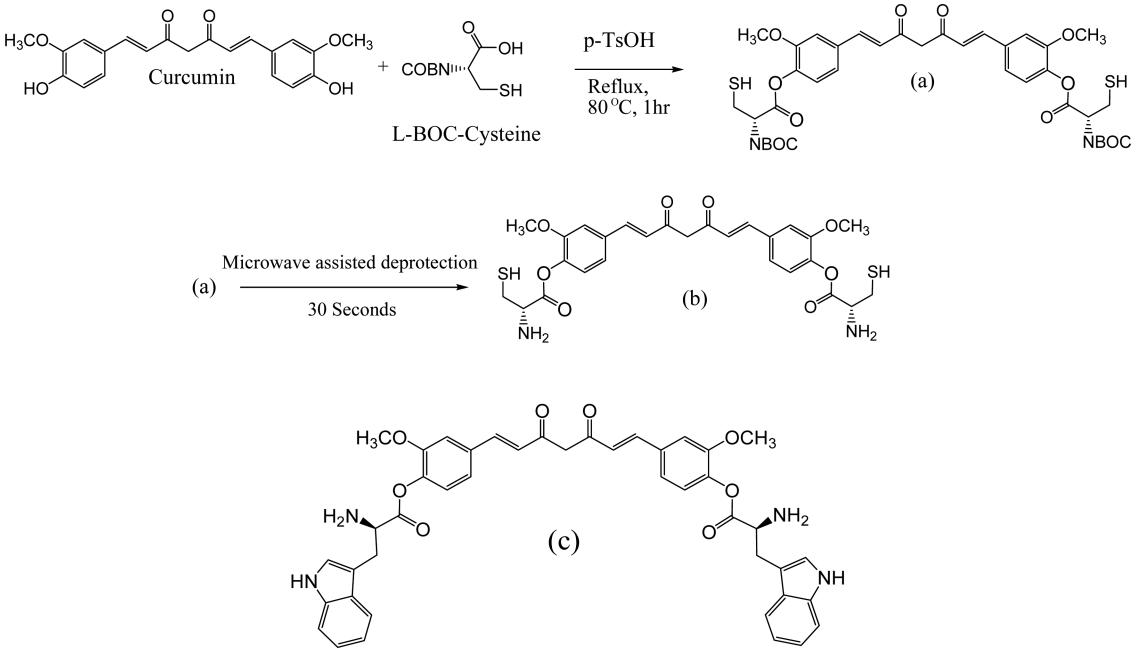

sensing experiments, the UV−vis spectra of the synthesized CC and CT were recorded and compared with curcumin, PA, Cys and Tryp. Curcumin shows a strong absorbance at about 380 nm which is due to $\pi-\pi^*$ transition of the extended conjugated chromophore (refer Supporting Information Figure S4A). The solution of curcumin exhibits a bright yellow color due to the low $\pi-\pi^*$ transition of the chromophore. The peak undergoes redshift to 420 nm after formation of CC and CT. This is attributed due to the fact that binding with the amino acids results in extension of conjugation which decreases the energy level of the π^* orbital. Hence, electronic excitation in CC and CT can occur by absorbing lower amount of energy from the UV light. On the other hand, virgin Cys and Tryp possesses absorbance below 300 nm and for PA the value is about 350 nm. Incremental addition of PA increases the absorbance of CC and CT at 350 (refer Supporting Information Figure S4B and C). At 430 nm, the value does not increase upon addition of PA and hence preferred as the λ_{ex} for the fluorescence sensing experiments. The aqueous solutions of these compounds are acidic in nature with pH about 4. Here, both CC and CT shows very weak emission band located at about 540 and 535 nm, respectively, when λ_{ex} is 430 nm. The nonfluorescent nature of the probes is believed to be due to intramolecular quenching. But with increasing concentration of PA, the fluorescence intensity of CC and CT regularly increases without any shift in the spectral energies as shown in Figure 1 A and B. This fluorescence turn on is very efficient and both the compounds achieves about 26.5 fold enhancement in their fluorescence intensity when the PA concentration reaches 70 nM. The value is considerably higher in comparison to the recent reported works.[13,18] Here, the concentration of the probes were maintained at 0.1 mM. The study has also been carried out with 0.2 mM, 0.01 mM and 0.001 mM concentration of CC and CT, and the results are presented in Supporting Information Figure S5. The distinct fluorescence enhancement in CC and CT can be witnessed by necked eye under normal light and UV light irradiation as shown in Figure 1C and D.

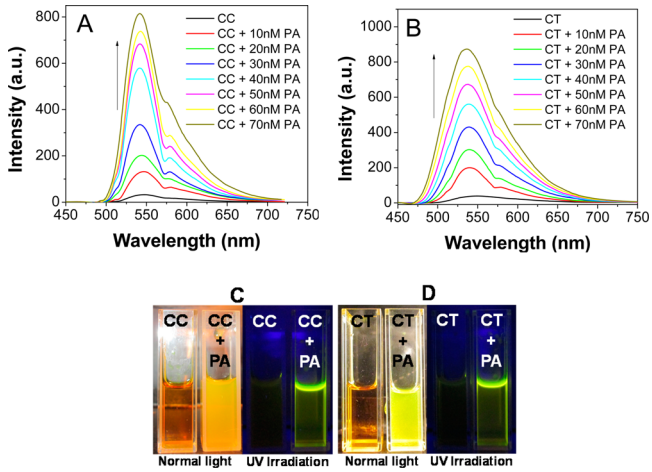

Figure 1. Fluorescence titration of (A) CC (0.1 mM) and (B) CT (0.1 mM) at with increasing concentration of PA in aqueous medium (pH 4) with λ_{ex} 430 nm. Images of (C) CC, CC + PA and (D) CT, CT + PA under normal light and UV irradiation (365 nm).

The sensor−analyte solution shows green fluorescence under 365 nm UV light irradiation. While, virgin curcumin, Cys and Tryp are fluorescence irresponsive to PA at the same λ_{ex} (refer Supporting Information Figure S6). To check the selectivity for PA, the photonics of CC and CT were investigated in the presence of similar NACs like TNT, DNSA, NB, ONP, and PNP and plotted in Figure 2A and B. Both the probes are fluorescence irresponsive to these NACs which in turn ascertain their selectivity toward PA. The corresponding images under UV light irradiation are shown in Figure 2C and D. The interference of these NACs in 1:1 molar ratios with PA is also very negligible as evident from the histogram shown in Figure 2E and F. Along with other NACs, the selectivity and interference tests for common laboratory chemicals including methanol, ethanol, acetone, THF, and acetic acid were also investigated. The effect of these chemicals toward the sensitivity

DOI: 10.1021/acsami.5b01102
ACS Appl. Mater. Interfaces 2015, 7, 11195−11202

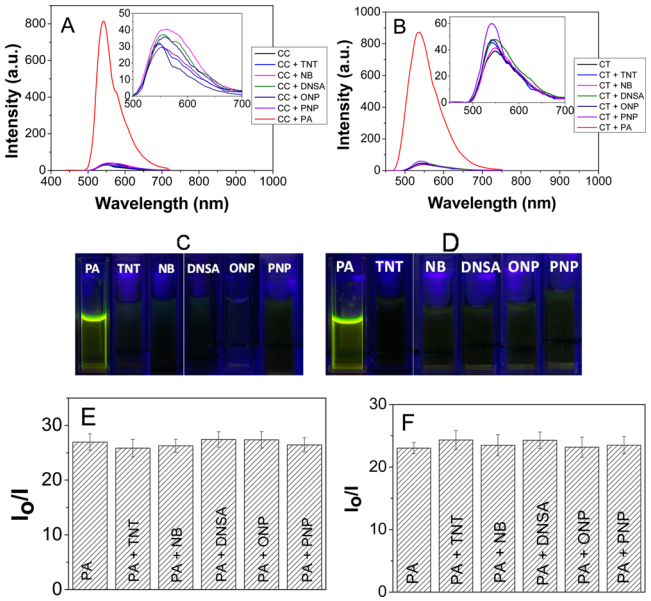

Figure 2. Fluorescence spectra of (A) CC and (B) CT in the presence of 70 nM of PA and the interference of similar NACs toward the detection of PA. Images of (C) CC and (D) CT with different NACs under UV lamp (365 nm). Histogram for the interference of other NACs toward the detection of PA by (E) CC and (F) CT in aqueous media.

for PA is very minimal (refer Supporting Information Figure S7). The probes show prompt fluorimetric response to PA addition as its response time is <30 s, which implies that it is useful for quick detection of PA in aqueous media. Such high selectivity, low interference of similar analyte and quick response to the analyte is important for an efficient sensing process. In addition to the electron withdrawing NACs, the fluorescence behavior of the probes were investigated for basic chemicals like ammonia, aniline and pyridine (refer Supporting Information Figure S8). Interestingly, there was no significant fluorescence turn on for such chemicals. Also, the effect of varying pH toward the sensitivity for PA was investigated. Both the probes are efficient only at acidic pH (refer Supporting Information Figure S9 and Figure 10).

The calibration curves for CC and CT with the increasing concentration of PA were constructed as shown in Figure 3. A statistically applicable linear relationship was observed in between the fluorescence enhancement and the concentration of the analyte which indicates that the two probes are applicable for PA sensing. From the calibration curves the LOD were calculated using the formula LOD = 3.3 σ/S, where, "σ" is the

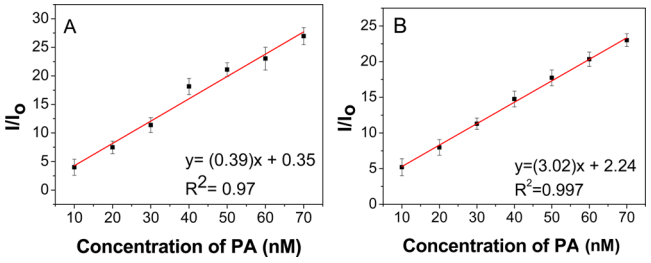

Figure 3. Calibration curves for A. CC and B. CT with increasing concentration of PA. The error bars indicates the standard deviation of three replicate measurements.

relative standard deviation and 'S' is the slope of the calibration curve. It was found that the LOD of CC and CT can reach as low as 13.51 nM and 13.54 nM of PA respectively. These values are significantly lower compared to that of the previously reported aqueous phase fluorimetric detection of PA (discussed later in the comparative study).

With reference to the Scheme 4, the sensing strategy and selectivity for PA is based on the electrostatic interaction

Scheme 4. Electrostatic interaction of PA with (A) CC and (B) CT

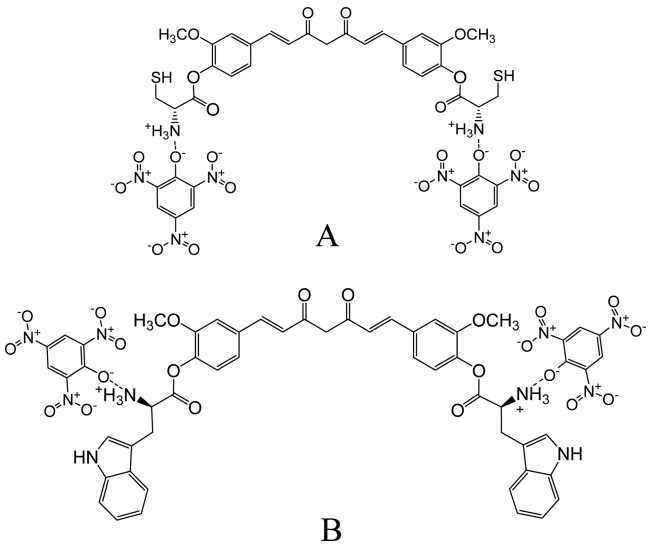

between the probes with PA. The phenolic group of PA is highly acidic due to the strong electron withdrawing effect of three NO_2 groups and hence efficiently interacts with the basic amine group of CC and CT. Such electrostatic interaction was recently reported by Sun et al., where the amine group of bovine serum albumin (BSA) selectively interacts with the picrate ion.[29] But, unlike the interaction with PA, conventional protonation process by acid treatment with 0.01 M HCl does not lead to fluorescence turn on of the probe. To gain further insight into the structural factors, we have compared the FT-IR spectra of CC and CT before and after the sensing experiments. The FT-IR spectra are presented in Supporting Information Figure S11. Here, initially the N−H bending vibration of CC and CT was observed at 1585 cm^{-1}, which is notably shifted to 1570 and 1561 cm^{-1} respectively after the interaction with PA. All other peak positions of CC and CT remains intact which indicates that these groups are not involved in the electrostatic interaction with PA.

To confirm the electrostatic interaction between the probes and the picrate ion, a significantly higher concentrated salt solution (0.1 M of $NaNO_3$) was added to the probes and then their fluorescence activity toward PA (70 nM) were checked. Interestingly, it was observed that, in the presence of a concentrated salt the fluorescence turn on toward PA is very week compared to that without salt addition (Figure 4). This can be demonstrated with the help of salt screening effect at concentrated $NaNO_3$ solution. Such effects are considerably higher at significantly greater concentration of the added salt compared to the concentration of the analyte.[30] It is reported that, introduction of such salts hinders the association of the analyte with the probes due to electrostatic reasons. Also, at higher concentration of the salt the metal cation (Na^+) may

DOI: 10.1021/acsami.5b01102
ACS Appl. Mater. Interfaces 2015, 7, 11195−11202

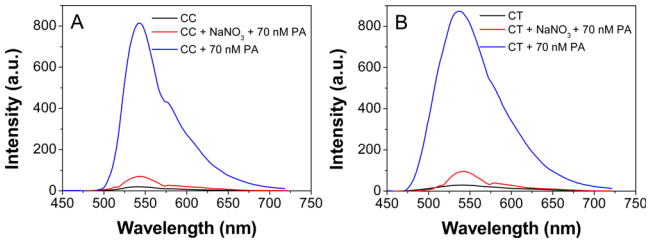

Figure 4. Fluorescence spectra of (A) CC and (B) CT in the presence of 70 nM of PA and (0.1 M $NaNO_3$ + 70 nM PA) solution.

form soluble salt with the picrate ion. Thus, picrate ion is no longer able to interact with the probes which directly influence on the fluorescence properties.

In the present system, the electrostatic interaction causes strong association of the sensor and analyte molecules, which is augmented by the DLS measurements, as shown in Figure 5. Initially, the average particle size of CC was about 823 nm and increased to about 1485 nm after association with PA molecules. For CT, the initial and final average particle size was found to be about 823 and 1368 nm, respectively. Such particle aggregation is the main reason for fluorescence turn on which is termed as aggregation induced emission (AIE). With the help of DLS measurements, it was observed that introduction of PA notably changes the zeta potential (ζ) values of the probes (refer to Supporting Information Figure S12). Here, PA possesses a negative ζ value of about −16.7 mV. Initially, CC and CT shows positive ζ value of about +15.4 and +19.34 mV respectively, which changes to about −0.96 and −1.3 mV after the interaction with PA. Such a notable change in the zeta potential values of the probes is a strong evidence of the electrostatic interaction between the probes and the analyte. It is well established that aggregation can be induced by electrostatic interaction, coordination, hydrophobic interaction, steric hindrance, or the influence of polarity and viscosity etc.[31] Tang et al. for the first time reported that restriction of intramolecular rotation in the aggregates is the main cause of AIE. While, unhindered intramolecular rotations in the free state leads to nonradiative decay.[32] We have carried out solid state fluorescence sensing experiments for the CC and CT treated with PA. Here, the aqueous samples were vacuum-dried and their fluorescence spectra were recorded using the same parameters. In both the cases, fluorescence turn on toward PA occurs very efficiently as shown in Figure 6. It is well-known that, in aggregated solid state the nonradiative intramolecular vibrational and rotational motions are restricted, which causes fluorescence enhancement.[33]

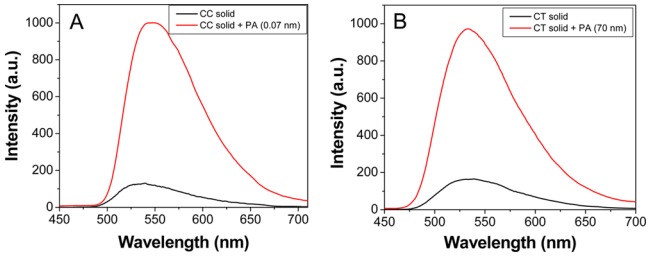

Figure 6. Solid-state fluorescence spectra of (A) CC and (B) CT in the presence of PA at λ_{ex} 430 nm.

In support of the DLS results, optical microscopy has also provided necessary information regarding the change in the particle size which is very important in the present context of the sensor system. Under optical microscope, the particles of the sensor−analyte systems (CC + PA and CT + PA) are largely aggregated resulting into significantly bigger sized particles compared to that of the probes alone (Figure 7).

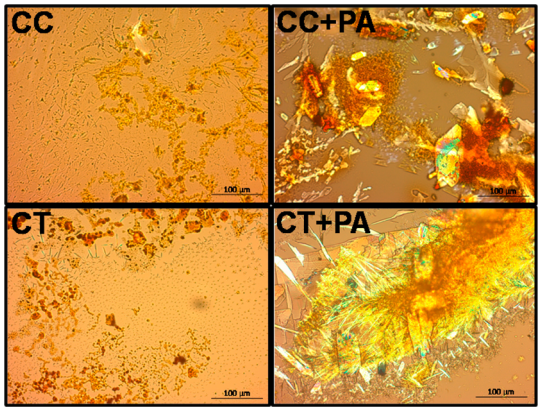

Figure 7. Images of CC, CC + PA, CT, and CT + PA under optical microscope.

This clearly reveals that AIE is the key reason for fluorescence turn on sensing of PA. The fluorescence turn on in these aggregated systems was clearly observed under fluorescence microscope as shown in Figure 8. While illumination with rhodamine monochromatic light, the aggregated systems shows strong red emission which was not observed for the CC and

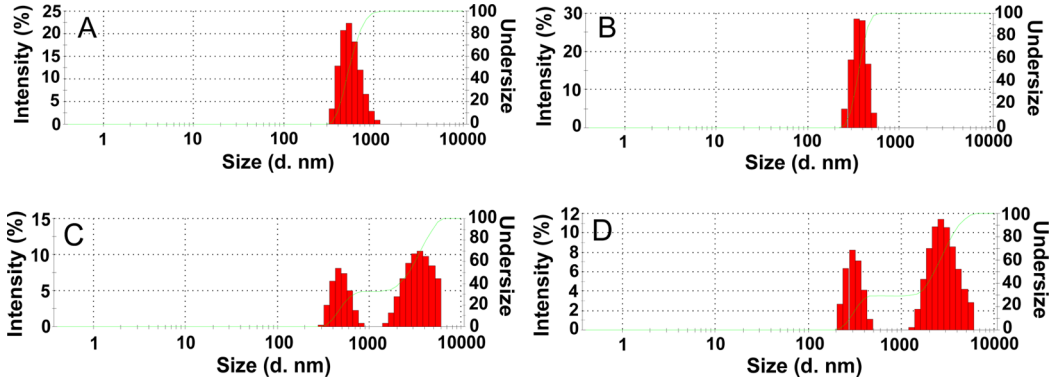

Figure 5. DLS of (A) CC, (B) CT, (C) CC + PA, and (D) CT + PA in aqueous media.

DOI: 10.1021/acsami.5b01102
ACS Appl. Mater. Interfaces 2015, 7, 11195−11202

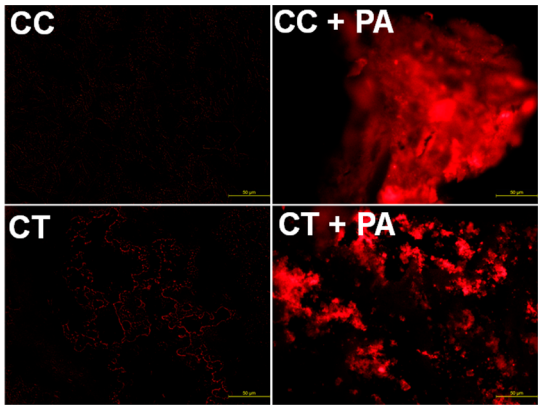

Figure 8. Images of CC, CC + PA, CT, and CT + PA under fluorescence microscope.

CT without PA. This result supports the solid state florescence turn on spectra of the probes after sensing PA.

Fluorescence Sensing in Real Sample. To investigate the potential practical application of the proposed method, the fluorescence response of the probes for PA were tested in real samples. Here, the real samples were prepared by using pond water, tap water, and drinking water spiked with PA and fluorescence activities for these samples were checked. It was found that, the fluorescence turn on for these samples follow the same pattern that has been observed for laboratory samples. All the fluorescence spectra for real sample analysis are presented in Figure 9. Again, in environmental samples, there

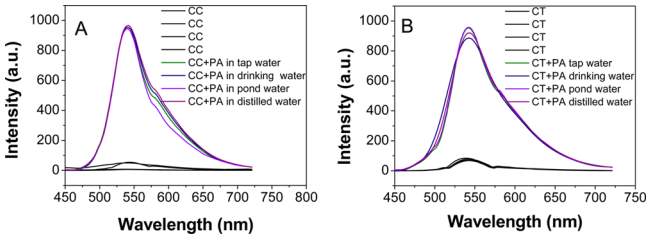

Figure 9. Fluorescence response of (A) CC and (B) CT toward PA in real samples.

can be impurities due to the presence of different metal ions in low concentrations. Therefore, to further investigate the practical application, we have carried out fluorescence sensing for PA in the presence of different metal ions. Figure 10 depicts that neither the probes shows fluorescence response to such metal ions nor the presence of such metal ions (0.1 μM) alter the sensitivity toward PA. This is due to the absence of proper binding sites at the sensing materials for metal ions which finally helps in selectively sensing PA. In addition to the selectivity for PA, the photostability and required time for sensing is also very important for practical application. As mentioned earlier, the fluorescence response for PA is very instant and hence applicable for quick detection process. In general, the organic fluorescence are not photostable and their fluorescence activity changes with time. In the present context, the photostability of the system is another advantage for the application as the enhanced fluorescence intensity in presence PA do not decline with time scale as demonstrated in Figure 11.

Comparative Study of Our System with Previously Reported PA Sensors. In comparison to the previously reported works, the very first advantage of our method arises

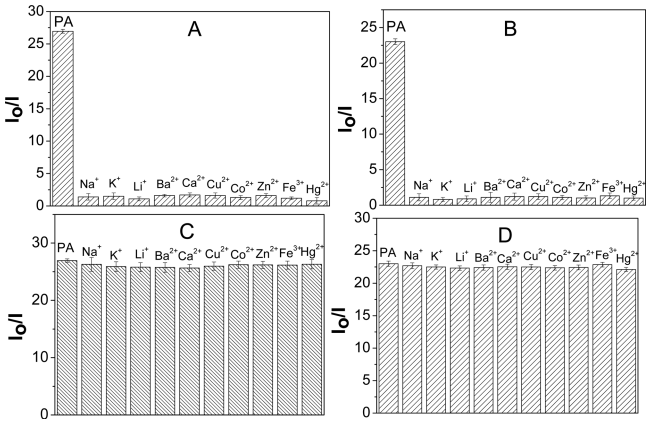

Figure 10. Histogram for the fluorescence behavior of (A) CC and (B) CT toward PA and metal ions. Interference of metal ions toward the sensitivity of (C) CC and (D) CT for PA.

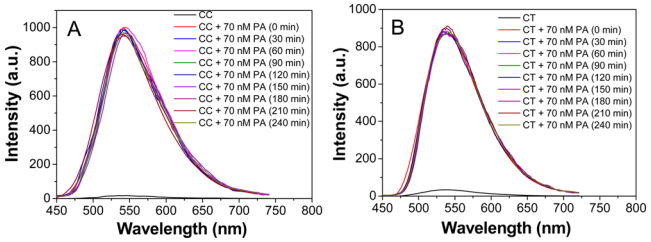

Figure 11. Photostability test: Fluorescence spectra of (A) CC and (B) CT in the presence of 70 nM of PA in aqueous media at different time scale. The spectra are almost same for about 240 min.

from the perspective of developing biobased probes for the detection of PA. Use of such chemicals are more preferable compared to the other probes developed by using quantum dots, other organic chemicals, graphene, etc., which are regarded as toxic materials. The method is efficient in aqueous medium which is important for practical applications of sensing PA in real samples. Also, the method provides better sensitivity in terms of higher fluorescence enhancement and lower LOD as shown in the Table 1.

CONCLUSION

The results of the steady state fluorescence emission indicate that the two biobased materials developed from curcumin and amino acids are efficient in selective, sensitive and instant detection of PA in aqueous media. Here, L-BOC cysteine and L-BOC Tryptophan are used as the required amino acids to prepare the probes. The probes are primarily non fluorescent in nature and reach about 26.5-fold fluorescence enhancement at PA concentration as low as 70 nM. This fluorescence enhancement is remarkably higher in comparison to the reported processes for the detection of PA. The limit of detection for curcumin−cysteine and curcumin−tryptophan were calculated to be 13.51 and 13.54 nM of PA, respectively. The electrostatic interaction between the probes and the analyte plays the determinative role in fluorescence turn on by the process aggregation induced emission. Furthermore, the materials are capable of sensing PA in real samples, which is of utmost important in terms of practical application. Thus, in a nutshell, the two biobased materials act as very simple aqueous sensors to picric acid in both laboratory and real environmental samples.

DOI: 10.1021/acsami.5b01102
ACS Appl. Mater. Interfaces 2015, 7, 11195−11202

Table 1. Comparative Study of the Present System with Previously Reported Systems

serial no.[a]	material	method	medium	LOD
1	bovine serum albumin (BSA)	fluorescence turn off	aqueous	17.2 nM
2	graphene oxide methyl cellulose hybrid	fluorescence turn off	aqueous	2 ppm
3	rhodamine 6G hydrazide with 4-*N*,*N*-dimethylaminobenzaldehyde	fluorescence turn on	aqueous	45 nM
4	sodium dodecyl sulfate (SDS)	fluorescence turn off	aqueous	1 μM
5	functionalized reduced grapheme oxide	fluorescence turn off	aqueous	125 ppb
6	DNSA-SQ	ratiometric	aqueous	70 nM
7	phosphole oxide	fluorescence turn off	10% THF in water	2.03 mM
8	BODIPY	fluorescence turn on	CH_3CN–H_2O (9:1)	162 ppb
9	tripyrenyltruxene	fluorescence turn off	10% aq. THF	0.15 ppm
10	isobenzotriazolophanes	fluorescence turn off	Cyclohexane	19 ppm
11	9,10-dibromoanthracene derivative	fluorescence turn off	DMA or CH_2Cl_2	in ppb
12	benzimidazole derivatives	fluorescence turn off	THF	50 ppb
13	tris-imidazolium derivatives	fluorescence turn off	DMSO	467 and 354 ppb
14	curcumin–cysteine (CC) curcumin–tryptophan (CT)	fluorescence turn on	aqueous	13.54 nM and 13.51 nM of PA

[a] **1**, ref 29; **2**, ref 34; **3**, ref 12; **4**, ref 35; **5**–**7**, ref 36–38; **8**, ref 13; **9**, **10**, ref 39, 40; **11**, ref 14; **12**, **13**, ref 41, 42; **14**, the present work.

■ ASSOCIATED CONTENT

Supporting Information

FT-IR spectral analysis of curcumin, CC, and CT, NMR analysis, MS analysis with possible fragments, elemental analysis, UV–vis spectral analysis, fluorescence spectra of CC and CT at different concentrations, fluorescence sensing of PA at different concentrations of CC and CT, fluorescence spectra of curcumin, Cys, and Tryp in the presence of PA, selectivity and interference tests for common laboratory chemicals, fluorescence spectra of CC and CT in the presence of basic chemicals, fluorescence spectra of CC and CT in the presence of PA in basic pH, fluorescence spectra of CC and CT in the presence of 70 nM of PA with varying pH, FT-IR spectral analysis of CC and CT after sensing PA, and DLS measurements. The Supporting Information is available free of charge on the ACS Publications website at DOI: 10.1021/acsami.5b01102.

■ AUTHOR INFORMATION

Corresponding Author

*E-mail: neelot@iasst.gov.in. Phone: +91(0361)2270084. Fax: (0361)2740659.

Notes

The authors declare no competing financial interest.

■ ACKNOWLEDGMENTS

This work is financially supported by DeitY, Govt. of India. The authors also acknowledge, Sudesna Chakravarty, Dr Nandana Bhardwaj, R. Elancheran, and Kiranjyoti Mohan for their help during the work. We are grateful to the reviewers for their critical comments to improve the manuscript.

■ REFERENCES

(1) Akhavan, J. *The Chemistry of Explosives*; 3rd ed.; Royal Society of Chemistry: Cambridge, U.K., 2011; Chapter 1, pp 1–22.
(2) Hamric, J. T. High Temperature Explosive System Containing Trinitromesitylene. United States Patent 3515604, June 2, 1970.
(3) Peng, Y.; Zhang, A. J.; Dong, M.; Wang, Y. W.A Colorimetric and Fluorescent Chemosensor for the Detection of an Explosive—2,4,6-Trinitrophenol (TNP). *Chem. Commun.* **2011**, *47*, 4505–4507.
(4) Hou, X. G.; Wu, Y.; Cao, H. T.; Sun, H. Z.; Li, H. B.; Shan, G. G.; Su, Z. M. A Cationic Iridium(III) Complex with Aggregation-Induced Emission (AIE) Properties for Highly Selective Detection of Explosives. *Chem. Commun.* **2014**, *50*, 6031–6034.
(5) Sohn, H.; Calhoun, R. M.; Sailor, M. J.; Trogler, W. C. Detection of TNT and Picric Acid on Surfaces and in Seawater by Using Photoluminescent Polysiloles. *Angew. Chem., Int. Ed.* **2001**, *40*, 2104–2105.
(6) McQuade, D. T.; Pullen, A. E.; Swager, T. M. Conjugated Polymer-Based Chemical Sensors. *Chem. Rev.* **2000**, *100*, 2537–2574.
(7) Germain, M. E.; Knapp, M. J. Optical Explosives Detection: From Color Changes to Fluorescence Turn-on. *Chem. Soc. Rev.* **2009**, *38*, 2543–2555.
(8) Shanmugaraju, S.; Joshi, S. A.; Mukherjee, P. S. Fluorescence and Visual Sensing of Nitroaromatic Explosives Using Electron Rich Discrete Fluorophores. *J. Mater. Chem.* **2011**, *21*, 9130–9138.
(9) Lee, Y. H.; Liu, H.; Lee, J. Y.; Kim, S. H.; Kim, S. K.; Sessler, J. L.; Kim, Y.; Kim, J. S. Dipyrenylcalix[4]arene—A Fluorescence-Based Chemosensor for Trinitroaromatic Explosives. *Chem.—Eur. J.* **2010**, *16*, 5895–5901.
(10) Yang, J. S.; Swager, T. M. Fluorescent Porous Polymer Films as TNT Chemosensors: Electronic and Structural Effects. *J. Am. Chem. Soc.* **1998**, *120*, 11864–11873.
(11) Toal, S. J.; Trogler, W. C. Polymer Sensors for Nitroaromatic Explosives Detection. *J. Mater. Chem.* **2006**, *16*, 2871–2883.
(12) Gandhi, S.; Balasubramanian, V.; Duraisamy, C. Rhodamine Based Selective Turn-on Sensing of Picric Acid. *R. Soc. Chem. Adv.* **2014**, *4*, 30828–30831.
(13) Madhu, S.; Bandela, A.; Ravikanth, M. BODIPY Based Fluorescent Chemodosimeter for Explosive Picric Acid in Aqueous Media and Rapid Detection in the Solid State. *R. Soc. Chem. Adv.* **2014**, *4*, 7120–7123.
(14) Gole, B.; Shanmugaraju, S.; Bar, A. K.; Mukherjee, P. S. Supramolecular Polymer for Explosives Sensing: Role of H-bonding in Enhancement of Sensitivity in the Solid State. *Chem. Commun.* **2011**, *47*, 10046–10048.
(15) Bhalla, V.; Gupta, A.; Kumar, D.; Rao, S. S.; Prasad, S. K. Self-Assembled Pentacenequinone Derivative for Trace Detection of Picric Acid. *ACS Appl. Mater. Interfaces* **2013**, *5*, 672–679.
(16) Meaney, M. S.; Mcguffin, V. L. Investigation of Common Fluorophores for the Detection of Nitrated Explosives by Fluorescence Quenching. *Anal. Chim. Acta* **2008**, *610*, 57–67.
(17) Yunsheng, X.; Lei, S.; Changqing, Z. Turn-On and Near-Infrared Fluorescent Sensing for 2, 4, 6-Trinitrotoluene Based on Hybrid (Gold Nanorod)–(Quantum Dots) Assembly. *Anal. Chem.* **2011**, *83*, 1401–1407.
(18) Zhang, K.; Zhou, H.; Mei, Q.; Wang, S.; Guan, G.; Liu, R.; Zhang, J.; Zhang, Z. Instant Visual Detection of Trinitrotoluene Particulates on Various Surfaces by Ratiometric Fluorescence of Dual-Emission Quantum Dots Hybrid. *J. Am. Chem. Soc.* **2011**, *133*, 8424–8427.

DOI: 10.1021/acsami.5b01102
ACS Appl. Mater. Interfaces 2015, 7, 11195–11202

(19) Freeman, R.; Finder, T.; Bahshi, L.; Gill, R.; Willner, I. Functionalized CdSe/ZnS QDs for the Detection of Nitroaromatic or RDX Explosives. *Adv. Mater.* **2012**, *24*, 6416−6421.
(20) Nagarkar, S. S.; Joarder, B.; Chaudhari, A. K.; Mukherjee, S.; Ghosh, S. K. Highly Selective Detection of Nitro Explosives by a Luminescent Metal−Organic Framework. *Angew. Chem., Int. Ed.* **2013**, *52*, 2881−2885.
(21) Zhang, S.; Ding, L.; Lu, F.; Liu, T.; Fang, Y. Fluorescent Film Sensors Based on SAMs of Pyrene Derivatives for Detecting Nitroaromatics in Aqueous Solutions. *Spectrochim. Acta, Part A* **2012**, *97*, 31−37.
(22) Wang, X.; Guo, Y.; Li, D.; Chen, H.; Sun, R. C. Fluorescent Amphiphilic Cellulose Nanoaggregates for Sensing Trace Explosives in Aqueous Solution. *Chem. Commun.* **2012**, *48*, 5569−5571.
(23) Sarkar, S.; Dutta, S.; Chakrabarti, S.; Bairi, P.; Pal, T. Redox-Switchable Copper(I) Metallogel: A Metal−Organic Material for Selective and Naked-Eye Sensing of Picric Acid. *ACS Appl. Mater. Interfaces* **2014**, *6*, 6308−6316.
(24) Wang, M.; Zhang, G.; Zhang, D.; Zhu, D.; Tang, B. Z. Fluorescent Bio/Chemosensors Based on Silole and Tetraphenylethene Luminogens With Aggregation-Induced Emission Feature. *J. Mater. Chem.* **2010**, *20*, 1858−1867.
(25) Kolev, T. M.; Velcheva, E. A.; Stamboliyska, B. A.; Spiteller, M. DFT and Experimental Studies of the Structure and Vibrational Spectra of Curcumin. *Int. J. Quantum Chem.* **2005**, *102*, 1069−1079.
(26) Gogoi, B.; Dutta, P.; Paul, N.; Dass, N. N.; Sarma, N. S. Polycurcumin Acrylate and Polycurcumin Methacrylate: Novel Bio-Based Polymers for Explosive Chemicals Sensor. *Sens. Actuators, B* **2013**, *181*, 144−152.
(27) Gogoi, B.; Sarma, N. S. Enhanced Fluorescence Quenching of Hemin Detected by a Novel Polymer of Curcumin. *R. Soc. Chem. Adv.* **2013**, *3*, 7747−7750.
(28) Chakravarty, S.; Saikia, D.; Sharma, P.; Adhikary, N. C.; Thakur, D.; Sarma, N. S. A Supramolecular Nanobiological Hybrid as a PET Sensor for Bacterial DNA Isolated from *Streptomyces sanglieri*. *Analyst* **2014**, *139*, 6502−6510.
(29) Sun, X.; Ma, X.; Kumar, C. V.; Lei, Y. Protein-Based Sensitive, Selective and Rapid Fluorescence Detection of Picric Acid in Aqueous Media. *Anal. Methods* **2014**, *6*, 8464−8468.
(30) Gang, H.; Haonan, P.; Taihong, L.; Meini, Y.; Yuan, Z.; Yu, F. A Novel Picric Acid Film Sensor via Combination of the Surface Enrichment Effect of Chitosan Films and the Aggregation-Induced Emission Effect of Siloles. *J. Mater. Chem.* **2009**, *19*, 7347−7353.
(31) Qiu, C. F.; Kwok, H. S.; Zhan, X. W.; Liu, Y. Q.; Zhu, d. b.; Tang, B. Z. Aggregation-Induced Emission of 1-Methyl-1,2,3,4,5-pentaphenylsilole. *Chem. Commun.* **2001**, 1740−1741.
(32) Hong, Y. N.; Lam, J. W. Y.; Tang, B. Z. Aggregation-Induced Emission: Phenomenon, Mechanism and Applications. *Chem. Commun.* **2009**, 4332−4353.
(33) Li, Y.; Li, F.; Zhang, h.; Xie, Z.; Xie, W.; Xu, X.; Li, B.; Shen, F.; Ye, L.; Hanif, M.; Ma, D.; Ma, Y. Tight Intermolecular Packing Through Supramolecular Interactions in Crystals of Cyano Substituted Oligo(*para*-Phenylenevinylene): A Key Factor for Aggregation-Induced Emission. *Chem. Commun.* **2007**, 231−233.
(34) Kundu, A.; Layek, R. K.; Nandi, A. K. Enhanced Fluorescent Intensity of Graphene Oxide−Methyl Cellulose Hybrid in Acidic Medium: Sensing of Nitro-aromatics. *J. Mater. Chem.* **2012**, *22*, 8139−8144.
(35) Ding, L.; Bai, Y.; Cao, Y.; Ren, G.; Blanchard, G. J.; Fang, Y. Micelle-Induced Versatile Sensing Behavior of Bispyrene-Based Fluorescent Molecular Sensor for Picric Acid and PYX Explosives. *Langmuir* **2014**, *30*, 7645−7653.
(36) Dinda, D.; Gupta, A.; Shaw, B. K.; Sadhu, S.; Saha, S. K. Highly Selective Detection of Trinitrophenol by Luminescent Functionalized Reduced Graphene Oxide through FRET Mechanism. *ACS Appl. Mater. Interfaces* **2014**, *6*, 10722−10728.
(37) Xu, Y.; Li, B.; Li, W.; Zhao, J.; Sun, S.; Pang, Y. "ICT-Not-Quenching" Near Infrared Ratiometric Fluorescent Detection of Picric Acid in Aqueous Media. *Chem. Commun.* **2013**, *49*, 4764−4766.
(38) Shiraishi, K.; Sanji, T.; Tanaka, M. Trace Detection of Explosive Particulates with a Phosphole Oxide. *ACS Appl. Mater. Interfaces* **2009**, *7*, 1379−1382.
(39) Samang, P.; Raksasorn, D.; Sukwattanasinitt, O.; Rashatasakhon, P. A Nitroaromatic Fluorescence Sensor from a Novel Tripyrenyl Truxene. *R. Soc. Chem. Adv.* **2014**, *4*, 58077−58082.
(40) Venkatesan, N.; Singh, V.; Rajakumar, P.; Mishra, A. K. Isobenzotriazolophanes: A New Class of Fluorescent Cyclophanes as Sensors for Aromatic Nitro Explosives−Picric Acid. *R. Soc. Chem. Adv.* **2014**, *4*, 53484−53489.
(41) Xiong, J. F.; Li, J. X.; Mo, G. Z.; Huo, J. P.; Liu, J. Y.; Chen, X. Y.; Wang, Z. Y. Benzimidazole Derivatives: Selective Fluorescent Chemosensors for the Picogram Detection of Picric Acid. *J. Org. Chem.* **2014**, *79*, 11619−11630.
(42) Roy, B.; Bar, A. K.; Gole, B.; Mukherjee, P. S. Fluorescent Tris-Imidazolium Sensors for Picric Acid Explosive. *J. Org. Chem.* **2013**, *78*, 1306−1310.

DOI: 10.1021/acsami.5b01102
ACS Appl. Mater. Interfaces 2015, 7, 11195−11202